Stabilization of Tie-Line Power Flow by Robust SMES Controller for Interconnected Power System With Wind Farms

Sanchai Dechanupaprittha, *Student Member, IEEE*, Komsan Hongesombut, *Member, IEEE*, Masayuki Watanabe, *Member, IEEE*, Yasunori Mitani, *Member, IEEE*, and Issarachai Ngamroo

***Abstract*—This paper presents the use of superconducting magnetic energy storage (SMES) with robust controllers for stabilization of tie-line power flow in a longitudinally interconnected power system with wind farms. The high penetration of wind power with abrupt changes causes fluctuations of tie-line power flow and significantly affects the effective use of transmission lines. A simultaneous active and reactive power control scheme of SMES including a characteristic of SMES coil current is employed for realizing a permissible range of SMES operation. Moreover, a multiplicative uncertainty model is considered in the parameter optimization of robust SMES controllers by using a heuristic method. Finally, simulation results are carried out to show the effectiveness and robustness under various situations.**

***Index Terms*—Power system stabilization, robust control, superconducting magnetic energy storage, wind farms.**

I. INTRODUCTION

NOWADAYS, the interest in wind power has been growing due to infinite availability and low impact to environment. However, wind power frequently changes and is hardly predictable. The high penetration of wind power with abrupt changes adversely affects power system operations. This can lead to severe problems, i.e., system frequency oscillations due to insufficient system damping, and/or violations of transmission capability margin due to severe fluctuations of tie-line power flow [1]. In multi-area power systems, not only a local frequency control is required in a given area but also fluctuations of tie-line power flow should be stabilized [2].

To overcome the problem, the superconducting magnetic energy storage (SMES) can be utilized as an effective device with the ability to swiftly exchange electrical energy with a power system. With proper control, SMES is capable of supplying and receiving the active and reactive power simultaneously as well as alleviating power system oscillations [3].

In this paper, a simultaneous active and reactive power control scheme of SMES including a characteristic of SMES coil current is employed for realizing a permissible range of SMES operation. Accordingly, the SMES coil current is controlled effectively within limits during operation. To enhance the power system stabilization, a multiplicative uncertainty model is embedded in the design of robust SMES controllers (RSMES). The 2nd order lead/lag compensator is employed for a controller and the control parameters are optimized using a heuristic method, i.e., hybrid tabu search and evolutionary programming (Hybrid TS/EP). The simulation studies on a longitudinally interconnected power system with six areas are carried out to show the effectiveness and robustness under various situations.

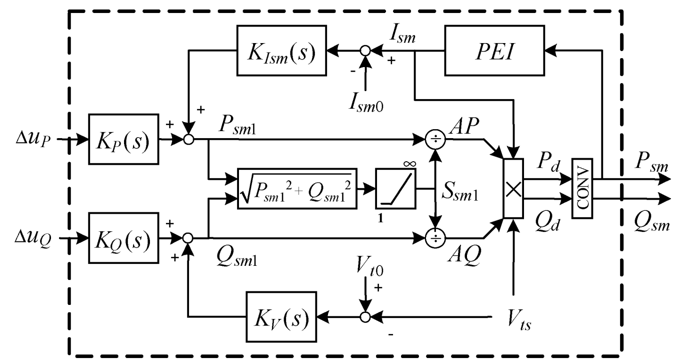

Fig. 1. SMES control scheme.

II. SMES CONTROL SCHEME

The SMES control scheme, as depicted in Fig. 1, is used in this paper. It is a simultaneous active and reactive power control scheme, which includes three controllers of $K_P(s)$, $K_Q(s)$ and $K_{Ism}(s)$, where, $K_P(s)$ and $K_Q(s)$ are the SMES active and reactive power controllers, respectively, and, $K_{Ism}(s)$ is the SMES coil current controller. In particular, the effect of SMES coil current (I_{sm}) is considered, since the dynamic behavior of I_{sm} significantly affects the overall performance of SMES. In practice, I_{sm} is not allowed to reach zero to prevent the possibility of discontinuous conduction under unexpected disturbances. On the other hand, high I_{sm}, which is above the maximum allowable limit, may lead to loss of superconducting properties. Based on the hardware operational constraints, the lower and upper coil current limits are considered and assigned as $0.30 I_{sm0}$ and $1.38 I_{sm0}$, respectively [4], where, I_{sm0} is an initial value of I_{sm}.

The PEI block in Fig. 1 is used to determine the present I_{sm} based on P_{sm}. In particular, I_{sm} can be calculated by

Manuscript received August 26, 2006.

S. Dechanupaprittha, M. Watanabe, and Y. Mitani are with the Graduate School of Engineering, Kyushu Institute of Technology, Fukuoka 804-8550, Japan (e-mail: e586406s@tobata.isc.kyutech.ac.jp).

K. Hongesombut is with the R&D Center, Tokyo Electric Power Company, Tokyo 230-8510, Japan (e-mail: Hongesombut.Komsan@tepco.co.jp).

I. Ngamroo is with the Faculty of Engineering, King Mongkut's Institute of Technology, Ladkrabang, Bangkok 10520, Thailand (e-mail: ingamroo@yahoo.co.th).

Digital Object Identifier 10.1109/TASC.2007.897846

(1) and (2) as follows,

$$Eout = \int P_{sm} dt \cdot S_{sm,base}, \tag{1}$$

$$I_{sm} = \sqrt{I_{sm0}^2 - 2E_{out}/\left(L_{sm} \cdot I_{sm,base}^2\right)}, \tag{2}$$

where, L_{sm} is the SMES coil inductance, (H); E_{out} is the SMES energy output, (J); $I_{sm,base}$ is the SMES current base, (A); and $S_{sm,base}$ is the SMES MVAbase, (MVA). Subsequently, the energy stored in the SMES unit (E_{sm}) and the initial $E_{sm}(E_{sm0})$ can be determined by (3) and (4) as follows,

$$E_{sm} = E_{sm0} - E_{out}, \tag{3}$$

$$E_{sm0} = 0.5 L_{sm} I_{sm0}^2 \cdot I_{sm,base}^2, \tag{4}$$

The desired SMES output active and reactive power (P_d and Q_d) can be expressed as

$$P_d = V_{ts} I_{sm} AP, \tag{5}$$

$$Q_d = V_{ts} I_{sm} AQ, \tag{6}$$

where, AP and AQ are the active and reactive power fractions, respectively. For simplicity, V_{ts} is a steady state bus voltage of SMES unit, (pu). The SMES output active and reactive power, i.e., P_{sm} and Q_{sm} are the output of the SMES controlled converter (CONV), which is represented by a first order time-lag compensator as follows,

$$P_{sm} = 1/(1 + 0.01s) P_d, \tag{7}$$

$$Q_{sm} = 1/(1 + 0.01s) Q_d. \tag{8}$$

In this paper, it is assumed that for a nominal condition the SMES unit should not supply/receive active and reactive power to/from the power system. On the other hand, the SMES unit should alleviate power system oscillations when being subjected to system disturbances.

III. Robust Controller Design

To enhance the power system stabilization, the structure of 2nd order lead/lag compensator is used in the design of $K_P(s)$ and $K_Q(s)$ controllers as

$$\Delta u_{CTL} = K_C \frac{sT_W}{1 + sT_W} \left[\frac{1 + sT_1}{1 + sT_2}\right] \left[\frac{1 + sT_3}{1 + sT_4}\right] \cdot \Delta u_{IN}, \tag{9}$$

where, Δu_{CTL} is the control output signal of controller; Δu_{IN} is the feedback input signal of controller; K_C is a controller gain; T_W is a washout time constant (s); and, T_1, T_2, T_3 and T_4 are time constants (s). Note that Δu_{IN} for $K_P(s)$ is the tie-line active power deviation (ΔP_{tie}), and Δu_{IN} for $K_Q(s)$ is the tie-line reactive power deviation (ΔQ_{tie}).

In this paper, T_W is set to 10s. The control parameters K_C, T_1, T_2, T_3 and T_4 are optimized using Hybrid TS/EP [5] based on the following objective function F,

$$\begin{aligned} \text{Min} \quad & F(K_C, T_i) = \varphi + \gamma, \\ \text{st.} \quad & K_{\min} \le K_C \le K_{\max}, \\ & T_{\min} \le T_i \le T_{\max}, \quad i = 1, \ldots, 4 \end{aligned} \tag{10}$$

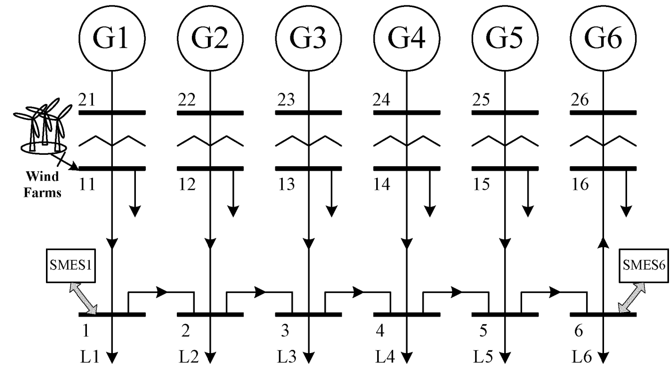

Fig. 2. Six-area interconnected power system with wind farms and SMESs.

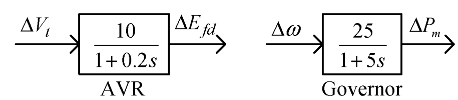

Fig. 3. AVR and Governor systems.

where, $K_{\min}, K_{\max}, T_{\min}$ and $T_{\max}$ are the minimum and maximum values of a controller gain and a time constant, respectively. φ is the difference between the actual and the desired damping ratios of the dominant power oscillation mode. γ is the normalized robustness index in terms of a multiplicative stability margin (MSM) [5]. It should be noted that the larger the MSM, the better the robust stability margin will be.

IV. Application to Interconnected Power System With Wind Farms

A. Study System

The interconnected power system as shown in Fig. 2 is employed in the study. The power system consists of six areas connected in a longitudinal configuration. Each area is represented by a 5th order generator model [6]. Fig. 3 depicts an automatic voltage regulator (AVR) and a governing system. It should be noted that the characteristic of a simple governor is used, since the tie-line power compensation by the SMES is apparently faster than that by the governor. This also implies that SMES and governing system can be coordinated properly. In addition, the dynamic of governor can be neglected in the design of RSMES. The area capacity ratio for areas 1 to 6 is 20:13.5:6.75:40:6.75:33 with a 1,000 MVA base. For study purpose, the electric power is transferred from areas 1 to 6. The wind farms are located in area 1 and have the maximum generation capacity of 500 MW. Based on the residue method [7], areas 1 and 6 are equipped with SMES for power system stabilization. The SMES has a specification of 800 MJ, 40 kA, 1,000 MVA.

B. Simulation Results and Evaluations

In this study, the RSMES are designed at the design operating condition (DOC). By using Hybrid TS/EP, the control parameters of $K_P(s)$ and $K_Q(s)$ controllers are optimized successfully based on the objective function (10) to yield the desired damping ratio of 0.055 and achieve the best obtainable MSM. Consequently, the robust control parameters are obtained

TABLE I
OPERATING CONDITIONS

	1.DOC (P_{tie} = 2.3)	2.LL (P_{tie} = 1.5)	3.HL (P_{tie} = 3.0)
G1	PG: 12, L1: 2.2 L11: 7+j0.7	PG: 8, L1: 1.5 L11: 5+j0.5	PG: 16, L1: 3.0 L11: 10+j1.0
G2	PG: 8.1, L2: 1.5 L12: 6.3+j0.6	PG: 5.4, L2: 1.0 L12: 4.2+j0.4	PG: 10.8, L2: 2.0 L12: 8.4+j0.8
G3	PG: 4.05, L3: 0.9 L13: 3.2+j0.3	PG: 2.7, L3: 0.6 L13: 2.1+j0.2	PG: 5.4, L3: 1.2 L13: 4.2+j0.4
G4	PG: 24, L4: 4.5 L14: 18.5+j1.8	PG: 16, L4: 3.0 L14: 13+j1.3	PG: 32, L4: 6.0 L14: 26+j2.6
G5	PG: 4.05, L5: 0.9 L15: 3.2+j0.3	PG: 2.7, L5: 0.6 L15: 2.1+j0.2	PG: 5.4, L5: 1.2 L15: 4.2+j0.4
G6	PG: 16.4, L6: 4.5 L16: 15.3+j1.5	PG: 11.55, L6: 3.0 L16: 10.2+j1.0	PG: 23.2, L6: 6.0 L16: 20.4+j2.0

PG: Generation (pu), L: Load (pu), Base: 1,000 MVA

TABLE II
DOMINANT MODES AND DAMPING RATIOS

Case	1.DOC (P_{tie} = 2.3)	2.LL (P_{tie} = 1.5)	3.HL (P_{tie} = 3.0)
No SMES	-0.074+j2.713; +0.027 -0.104+j3.679; +0.028	-0.114+j2.914; +0.039 -0.154+j3.894; +0.040	0.100+j2.387; **-0.042** -0.036+j3.413; +0.011
CSMES	-0.525+j3.299; +0.157 -0.366+j6.673; +0.055	-0.688+j3.763; +0.180 -0.438+j6.296; +0.069	-0.164+j2.744; +0.060 -0.095+j3.654; +0.026
RSMES	-0.400+j3.237; +0.123 -0.365+j6.651; +0.055	-0.471+j3.535; +0.132 -0.435+j6.278; +0.069	-0.106+j2.756; +0.039 -0.116+j3.740; +0.031

as follows.

$$\text{SMES1}: \quad K_P(s) = 1.02\frac{10s}{1+10s}\left[\frac{1+0.323s}{1+0.042s}\right]\left[\frac{1+0.287s}{1+0.068s}\right] \quad (11)$$

$$\text{SMES1}: \quad K_Q(s) = 2.00\frac{10s}{1+10s}\left[\frac{1+0.204s}{1+0.281s}\right]\left[\frac{1+0.620s}{1+0.180s}\right] \quad (12)$$

$$\text{SMES6}: \quad K_P(s) = 1.00\frac{10s}{1+10s}\left[\frac{1+0.425s}{1+0.233s}\right]\left[\frac{1+0.010s}{1+0.114s}\right] \quad (13)$$

$$\text{SMES6}: \quad K_Q(s) = 26.48\frac{10s}{1+10s}\left[\frac{1+0.097s}{1+0.019s}\right]\left[\frac{1+0.341s}{1+0.217s}\right] \quad (14)$$

For comparison purpose, the conventional SMES controllers (CSMES) are designed using the same method but the MSM is not considered in the design. In particular, the CSMES are also designed to yield the desired damping ratio of 0.055.

To evaluate the designed controller, three different operating conditions are employed as given in Table I, i.e., 1.DOC, 2.Light Load (LL) and 3.Heavy Load (HL). In particular, the tie-line power flows (P_{tie}) in all operating conditions are also different. In each case the eigenvalues of the power oscillation modes are evaluated as shown in Table II, however, only two dominant modes are given. This system has a dominant power oscillation mode with a long period which becomes unstable as the power flow becomes heavier.

TABLE III
MULTIPLICATIVE STABILITY MARGINS

Case	1.DOC (P_{tie} = 2.3)	2.LL (P_{tie} = 1.5)	3.HL (P_{tie} = 3.0)
CSMES	0.604	0.836	0.335
RSMES	0.858	1.202	0.403

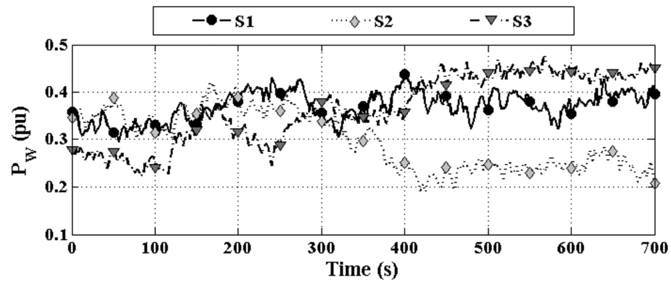

Fig. 4. Wind power generations [Base: 1000 MVA].

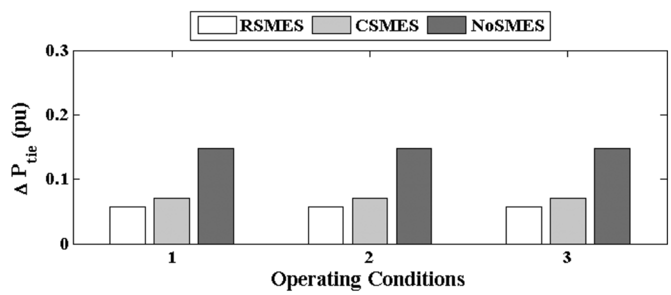

Fig. 5. Maximum deviations of P_{tie} with wind power S1 [Base: 1000 MVA].

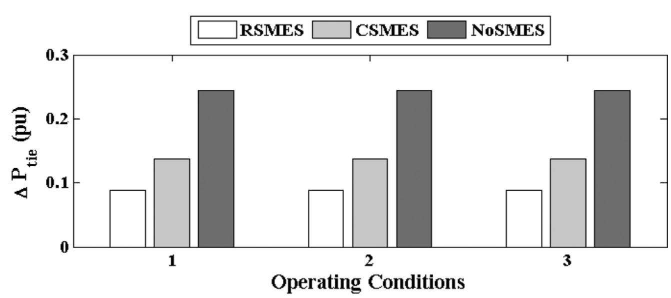

Fig. 6. Maximum deviations of P_{tie} with wind power S2 [Base: 1000 MVA].

As results, both RSMES and CSMES can significantly improve the system damping performance in all cases. In addition, MSMs are shown in Table III. In comparison with CSMES, the system with RSMES has higher MSMs. The higher MSM indicates the higher degree of system variations at which the system can persist without destabilized by unexpected disturbances.

Subsequently, nonlinear simulation studies are carried out to evaluate the effectiveness and robustness of tie-line power stabilization when the system is subjected to wind power fluctuations. The data of wind power (P_W) measured and collected from site are modified and employed to represent the wind power attached to area 1 at different situations as shown in Fig. 4. In particular, S1 represents the wind power with slightly changed generation. S2 represents the wind power with sudden decrease, and S3 represents the wind power with sudden increase.

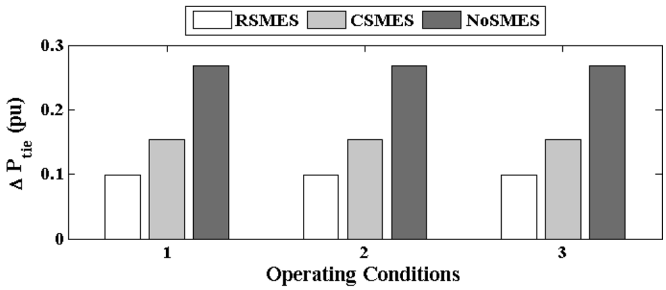

Fig. 7. Maximum deviations of P_{tie} with wind power S3 [Base: 1000 MVA].

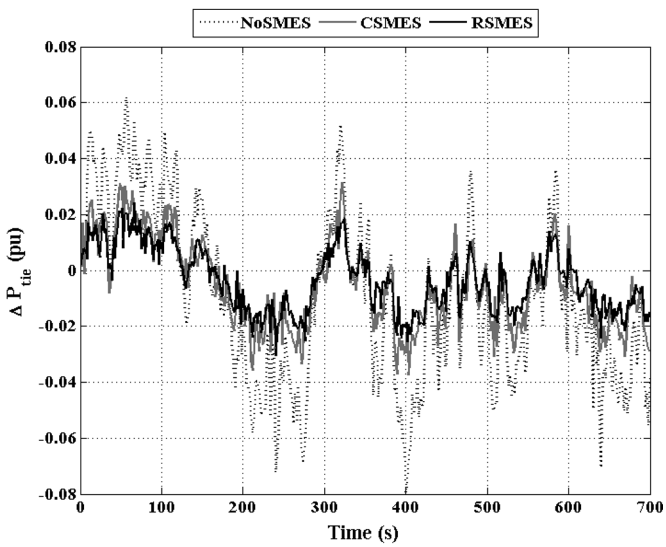

Fig. 8. System responses of P_{tie} in case HL with wind power S1.

As shown in Figs. 5–7, the maximum deviations of P_{tie} in different cases and wind power situations are presented. Fig. 5 shows the comparison when the wind power S1 is applied. The power system with CSMES and RSMES shows significantly the improvement of tie-line power flow. On the other hand, in case without SMES (NoSMES) fluctuations of P_{tie} are high, although the power system is still stable. Figs. 6 and 7 show the comparison when the wind powers S2 and S3 are applied, respectively. It is obvious that RSMES yield effectively the best performance in comparison with CSMES and NoSMES. This also implies that RSMES can retain satisfactorily the robust performance. Next, some nonlinear time-domain simulation results are illustrated to show the effectiveness and robustness of the designed controller. Fig. 8 shows the system responses of P_{tie} in case HL when the wind power S1 is applied. In comparison with NoSMES, the maximum deviations of P_{tie} in case of RSMES can be reduced by 62%, whereas in case of CSMES can be reduced by 53%. It should be noted that the dynamic of governor is also included in the time-domain simulation to show that SMES and governing system can properly work together.

Fig. 9 shows the system responses of I_{sm} of SMES1 and SMES6 in case HL when the wind power S1 is applied. Apparently, both I_{sm} of RSMES and CSMES can properly remain within the allowable limits. However, the fluctuation of I_{sm} in case of RSMES is larger. This is due to the fact that RSMES can appropriately supply and receive the larger amount of electrical energy with the power system. Accordingly, the stabilization of tie-line power flow by RSMES is superior to that by CSMES. In addition, it should be noted that the electrical energy stored in the SMES is also appropriately utilized due to the close correlation between E_{sm} and I_{sm}.

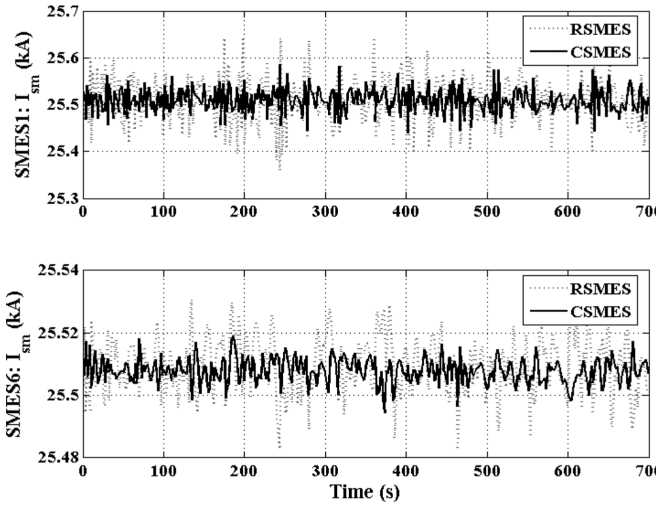

Fig. 9. System responses of I_{sm} in case HL with wind power S1.

V. Conclusion

In this paper, the use of robust SMES controller for stabilization of tie-line power flow in a longitudinally interconnected power system is presented. SMES is an effective device and can be applied to various applications in power systems. With proper controller design, SMES can be a promising solution for mitigating problems of tie-line power fluctuations due to adverse effects of wind farms in a power system. Moreover, by considering the robustness in the controller design, the robust SMES controller can robustly operate and maintain the effective use of transmission lines. Finally, simulation results exhibit and confirm the effectiveness and robustness in case of a power system with wind farms under various situations.

References

[1] J. G. Slootweg and W. L. Kling, "The impact of large scale wind power generation on power system oscillations," *Electric Power Systems Research*, vol. 67, no. 1, pp. 9–20, 2003.
[2] P. Kundur, *Power System Stability and Control*. New York: McGraw Hill, 1994, ch. 11.
[3] Y. Mitani, K. Tsuji, and Y. Murakami, "Application of superconducting magnetic energy storage to improve power system dynamic performance," *IEEE Trans. Power Systems*, vol. 3, no. 4, pp. 1418–1425, 1988.
[4] C. J. Wu and Y. S. Lee, "Application of superconducting magnetic energy storage unit to improve the damping of synchronous generator," *IEEE Trans. Energy Conversion*, vol. 6, no. 4, pp. 573–578, 1991.
[5] S. Dechanupaprittha, K. Hongesombut, M. Watanabe, Y. Mitani, and I. Ngamroo, "Design of robust SMES controller in a multimachine power system by using hybrid TS/EP," in *Proc. 15th Power Systems Computation Conference (PSCC05)*, Liege, Belgium, 2005.
[6] J. Machowski, J. Bialek, and J. R. Bumby, *Power System Dynamics and Stability*. New York: Wiley, 1997, ch. 10.
[7] N. Martin and L. T. G. Lima, "Determination of suitable locations for power system stabilizers and static var compensators for damping electromechanical oscillations in large power systems," *IEEE Trans. Power Systems*, vol. 5, no. 4, pp. 1455–1469, 1990.